

# *Staphylococcus aureus* virulence attenuation and immune clearance mediated by a phage lysin-derived protein

Hang Yang<sup>1</sup> , Jingjing Xu<sup>2</sup>, Wuyou Li<sup>2</sup>, Shujuan Wang<sup>1</sup>, Junhua Li<sup>1</sup>, Junping Yu<sup>1</sup>, Yuhong Li<sup>2\*</sup>  & Hongping Wei<sup>1,\*\*</sup> 

## Abstract

**New anti-infective approaches are much needed to control multi-drug-resistant (MDR) pathogens, such as methicillin-resistant *Staphylococcus aureus* (MRSA). Here, we found for the first time that a recombinant protein derived from the cell wall binding domain (CBD) of the bacteriophage lysin PlyV12, designated as V12CBD, could attenuate *S. aureus* virulence and enhance host immune defenses via multiple manners. After binding with V12CBD, *S. aureus* became less invasive to epithelial cells and more susceptible to macrophage killing. The expressions of multiple important virulence genes of *S. aureus* were reduced 2.4- to 23.4-fold as response to V12CBD. More significantly, V12CBD could activate macrophages through NF- $\kappa$ B pathway and enhance phagocytosis against *S. aureus*. As a result, good protections of the mice from MRSA infections were achieved in therapeutic and prophylactic models. These unique functions of V12CBD would render it a novel alternative molecule to control MDR *S. aureus* infections.**

**Keywords** anti-virulence therapy; bacteriophage lysin; cell wall binding domain; immune clearance; macrophage activation

**Subject Categories** Immunology; Microbiology, Virology & Host Pathogen Interaction

**DOI** 10.15252/emboj.201798045 | Received 18 August 2017 | Revised 20 June 2018 | Accepted 27 June 2018 | Published online 23 July 2018

**The EMBO Journal (2018) 37: e98045**

## Introduction

The emergence and increasing prevalence of bacterial strains that are resistant or tolerant to available antibiotics pose serious threats to the public health worldwide, demanding the discovery of new therapeutic approaches (Spellberg *et al*, 2008). Classical antibiotics are usually screened from natural products and compound libraries that have bacteriostatic or bacteriocidal activity against the whole

organisms (Martinez, 2008). However, bacterial pathogens can easily evolve to generate variants that withstand the immediate life-or-death pressure placed by such selected drugs, leading to the useless of these drugs, including the last-line antibiotics (Walsh, 2003; Projan & Bradford, 2007). Consequently, there is an urgent need for anti-infective agents with new modes of action different from classical antibiotics (Vicente *et al*, 2006).

Targeting bacterial virulence is an alternative approach that means to attenuate the pathogenesis of a target bacterium to aid clearance by the host immune defense (Cegelski *et al*, 2008; Rasko & Sperandio, 2010). Bacterial pathogens usually express a large repertoire of different virulence factors that help them to survive under various conditions. In addition, bacterial pathogens evolve to use different factors to interplay with the host at different times over the course of a complex infectious cycle (Miller *et al*, 1989). Usually, the successful infection is a result of complicated interactions between the time-resolved factors' expression profile of the pathogen and its microenvironment encountered during infection, but not a single one (Monack *et al*, 2004; Thanert *et al*, 2017). Therefore, the anti-virulence strategy can target multiple therapeutic windows to intervene the outcome of an infection, such as targeting bacterial factors mediating adhesion to the host (Krachler & Orth, 2013), secretion systems (Baron, 2010), regulatory systems (Rasko *et al*, 2008), quorum-sensing signaling (Starkey *et al*, 2014), elements that involved in evading host defense (Wang *et al*, 2015), and toxin trafficking and function (Saenz *et al*, 2007).

Other strategies based on the opsonophagocytic activity of antibodies derived from passive or active immunity have also been pursued as promising options for bacterial diseases (DiGiandomenico & Sellman, 2015). Although successful for the treatment of several infections, such as pneumococcal pneumonia, meningococcal meningitis, and tuberculosis (Casadevall *et al*, 2004), the antibody-based therapies are not available yet for many notorious multi-drug-resistant (MDR) pathogens, for instance methicillin-resistant *Staphylococcus aureus* (MRSA). Encouragingly, several vaccine candidates, including a monoclonal antibody

<sup>1</sup> Key Laboratory of Special Pathogens and Biosafety, Center for Emerging Infectious Diseases, Wuhan Institute of Virology, Chinese Academy of Sciences, Wuhan, China

<sup>2</sup> The State Key Laboratory Breeding Base of Basic Science of Stomatology (Hubei-MOST) & Key Laboratory of Oral Biomedicine, Ministry of Education, School and Hospital of Stomatology, Wuhan University, Wuhan, China

\*Corresponding author. Tel: +86 27 87647443; Fax: +86 27 87647443; E-mail: 1004809372@whu.edu.cn

\*\*Corresponding author. Tel: +86 27 51861076; Fax: +86 27 87199492; E-mail: hpwei@wh.iov.cn

binding to *S. aureus* toxin, are currently in clinical trials (Hua et al, 2014; DiGiandomenico & Sellman, 2015; Giersing et al, 2016). A recent report also showed that chimeric antibodies by fusing IgG Fc with binding domains from cell wall hydrolases were found having opsonophagocytic activities against *S. aureus* in mice models (Raz et al, 2017), which may represent a new approach for developing therapeutic antibodies. However, opsonophagocytic antibodies that perform well in animal models may have rare or no protective efficacy in humans as evidenced by the failure of all previous *S. aureus* vaccines that have been proven to be protective in experimental models (Proctor, 2012; Jansen et al, 2013; Fowler & Proctor, 2014).

Lysins, expressed by bacteriophages to digest the host bacterial cell wall for the release of newly assembled progeny virions, have attracted much attention as alternative anti-infectives against infectious diseases (Nelson et al, 2012; Pastagia et al, 2013). Lysins can lyse the peptidoglycan layer of target bacteria, resulting in their death within minutes. Lysins are modular in structure with a peptidoglycan hydrolytic catalytic domain and a cell wall binding domain (CBD) recognizing the conserved element in wall carbohydrates of a target bacterium (Fischetti, 2005). Researchers have consensus on high affinity and low resistance of lysin CBDs. However, nothing is known about the effects of CBDs on virulence and infection of target pathogens so far.

In the present work, we found that a protein derived from CBD of lysin PlyV12 (Liu et al, 2015), not the whole lysin, has surprising anti-virulence capacity against methicillin-resistant *S. aureus* (MRSA). MRSA now represents an enormous public health burden that is not adequately addressed by current antibiotics (Boucher & Corey, 2008; DeLeo & Chambers, 2009; Tong et al, 2015). Here, we found for the first time that V12CBD could repress expression of *S. aureus* virulence genes, sensitize *S. aureus* to the killing of macrophage, promote phagocytosis of macrophage, and eventually protect mice from lethal MRSA infections in therapeutic and prophylactic models. Unlike current antibiotics, V12CBD can act not only on reducing virulence of bacteria, but also on activating host immunity. These unique functions would render V12CBD a novel molecule to control MDR *S. aureus* infections.

## Results

### Binding with V12CBD suppresses the invasion of *Staphylococcus aureus* to epithelial cell *in vitro*

V12CBD can bind to the cell wall of *S. aureus* to form complex (Dong et al, 2015), without interfering with the growth or the morphology of *S. aureus* (Appendix Fig S1). Because the primary site of *S. aureus* infection is often a breach in epithelial cells that may lead to colonization and internalization, causing acute and chronic infections, we tested whether V12CBD could inhibit adhesion and internalization of *S. aureus* into epithelial A549 cells. As shown in Fig 1A, the V12CBD-treated *S. aureus* cells displayed a reduced adhesion to A549 cells in comparison with the PBS-treated controls ( $1.09 \times 10^6$  CFU/well at 100  $\mu\text{g/ml}$  V12CBD vs.  $1.66 \times 10^6$  CFU/well in control,  $P < 0.05$ ). After using gentamycin to kill the bacteria adhered to the cell surface, the number of intracellular staphylococci

was also found lower in V12CBD-treated wells ( $2.67 \times 10^5$  CFU/well at 100  $\mu\text{g/ml}$  V12CBD vs.  $3.98 \times 10^5$  CFU/well in control,  $P < 0.05$ , Fig 1B). To assess the specificity of V12CBD, we examined the effects of V12CBD on the adhesion of *Listeria monocytogenes* (*Lmo*), *Streptococcus agalactiae* (*Sag*), and *Salmonella enteritidis* (*Sen*) to A549 cells. No significant differences were observed in V12CBD-treated groups and the PBS-treated groups (Fig 1C). Moreover, we tested the effects of the CBD (CBD511) of *Listeria* phage lysin Ply511 (Loessner et al, 1995), which has similar charge and hydrophobic properties to V12CBD ( $MW_{V12CBD} = 18.4$  kDa,  $pI_{V12CBD} = 9.96$ ,  $Z_{V12CBD} = +14.1$ ;  $MW_{CBD511} = 15.5$  kDa,  $pI_{CBD511} = 9.96$ ,  $Z_{CBD511} = +13.9$ ), on the adhesion and internalization of *S. aureus* N315 to A549 cells. Results showed that treatment with CBD511 reduces the adhesion and internalization of *Lmo* to A549 cells but not *S. aureus* (Appendix Fig S2). These results suggest that binding with V12CBD specifically suppresses adhesion and invasion of *S. aureus* to the epithelial cells.

### Binding with V12CBD sensitizes *Staphylococcus aureus* to killing by macrophages and attenuates the virulence of *S. aureus* in a mouse model

Because wall carbohydrates shield *S. aureus* from host immune defense and oxidant killing (O'Riordan & Lee, 2004), we next examined whether binding with V12CBD could promote phagocytosis of *S. aureus* by macrophages. After incubation with wheat germ agglutinin (WGA) conjugated, V12CBD (0, 25, 50, and 100  $\mu\text{g/ml}$ ) pretreated *S. aureus* N315 at 37°C for 1 h, macrophages RAW264.7 cells were treated with trypsin to detach the bacteria adhered on cell surface, washed, and analyzed by flow cytometry to determine the extent of phagocytosis (Fig 1D). The flow cytometry showed that V12CBD does not promote phagocytosis of WGA-conjugated *S. aureus* by macrophage RAW264.7 (Fig 1E). However, survival rate of V12CBD-treated *S. aureus* was ~ 4.3 times lower than that of the PBS-treated bacteria (24.6% at 100  $\mu\text{g/ml}$  V12CBD vs. 105.5% in control, Fig 1F) after incubation with RAW264.7 cells. When the concentration of V12CBD increased to 400  $\mu\text{g/ml}$ , the survival rate of V12CBD-treated *S. aureus* was ~ 10.3 times lower than that of the PBS-treated one (10.2% vs. 105.5%, Appendix Fig S3). Moreover, the fate of *S. aureus* after incubation with the peritoneal macrophages from BALB/c mouse showed similar survival trends (Fig 1G).

Since binding with V12CBD sensitized *S. aureus* to killing by macrophages in an *ex vivo* assay, a virulent MRSA isolate *S. aureus* T23 pretreated with various concentrations of V12CBD (0, 100, 200, and 400  $\mu\text{g/ml}$ ) was injected intraperitoneally to mice at a final dose of  $2.5 \times 10^8$  CFU/mouse. As shown in Fig 1H, the mice infected with PBS-treated *S. aureus* (bacteria alone,  $n = 5$ ) died within 1 day after the challenge, whereas the mice infected with V12CBD-treated *S. aureus* showed dose-dependent survival rates. Eighty percentages of the mice (4/5) were alive at day 10 after infection with 400  $\mu\text{g/ml}$  V12CBD-treated *S. aureus*.

### Binding with V12CBD suppresses multiple important virulence factors expressed by *Staphylococcus aureus*

To further understand the possible reasons behind the virulence attenuation, a RNA-Seq approach was used to investigate the impact

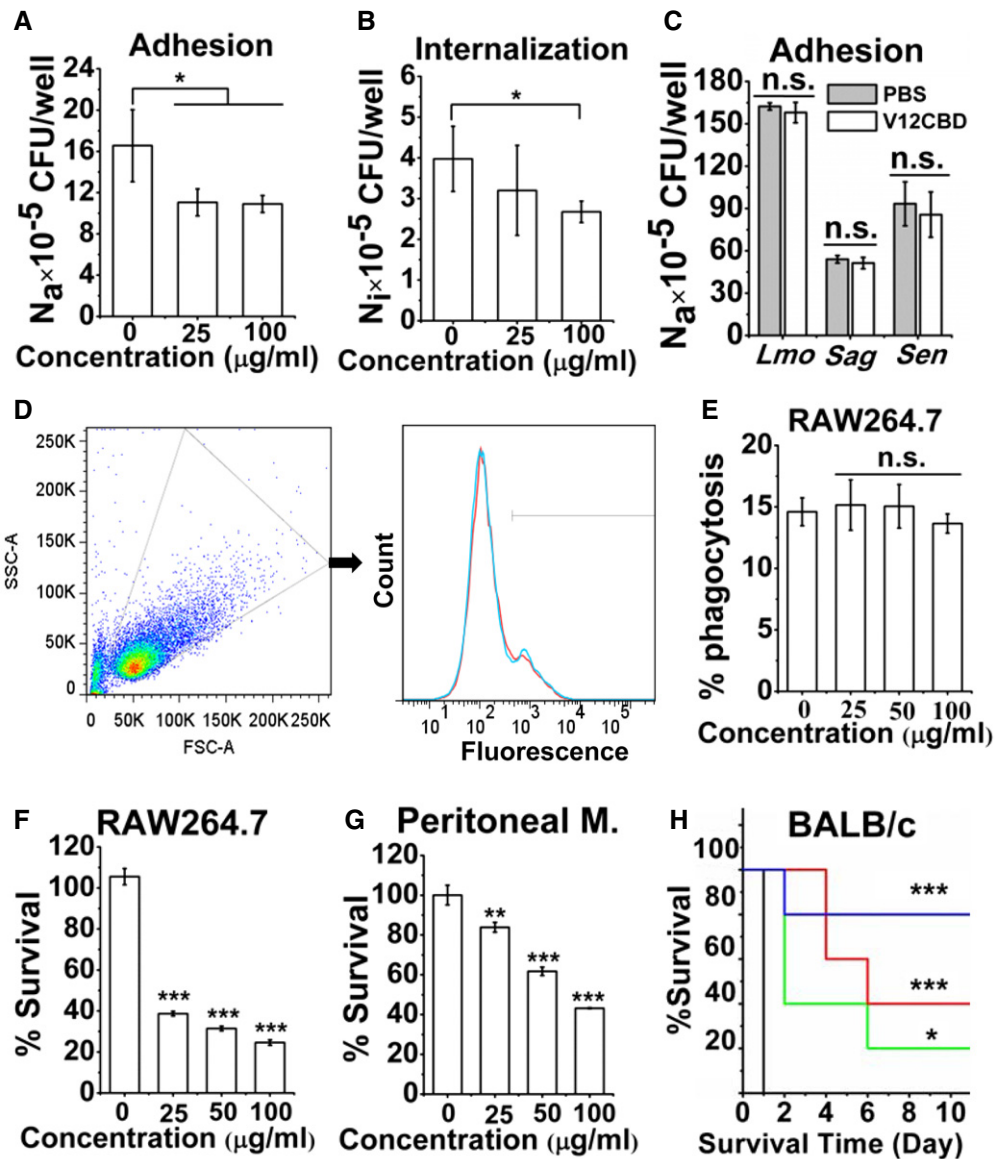


**Figure 1. Binding with V12CBD sensitizes immune clearance of *Staphylococcus aureus*.**

A, B Effects of V12CBD on the adhesion (A) and internalization (B) of *S. aureus* by A549 cells. The total number of viable bacteria within each well ( $N_t$ ) is determined by plating series dilutions on TSA plates. The internalized bacteria ( $N_i$ ) is determined by treating each well with 200  $\mu\text{g/ml}$  gentamycin for 2 h, followed by plating assay. The bacteria adhered on the cell surface ( $N_a$ ) is expressed as the difference between the total bacteria and the internalized ones ( $N_a = N_t - N_i$ ).  $n = 5$ . \* $P < 0.05$ .

C Effects of V12CBD on adhesion of *Listeria monocytogenes*, *Staphylococcus agalactiae*, and *Staphylococcus enteritidis* to A549 cells.  $n = 3$ . n.s., not significant.

D Example FACS plot for phagocytosis of *Staphylococcus aureus* by macrophages. WGA-conjugated *S. aureus* N315 is pretreated with various concentrations of V12CBD (red line) or PBS (cyan line) and then cocultured with macrophage RAW264.7 cells for 1 h at 37°C. After treatment with trypsin and washed with PBS at 300 g for six times, cells are analyzed using a BD LSRFortessa analyzer flow cytometer. Images shown are representative of two independent repeats ( $n = 3$  per group).

E Summary data of phagocytosis of *S. aureus* by macrophages. The extent of phagocytosis of each treatment is calculated using the CFlow software.  $n = 6$ . n.s., not significant.

F, G Effect of V12CBD on the susceptibility of *S. aureus* to killing by RAW264.7 and peritoneal macrophages. *Staphylococcus aureus* N315 is pre-bound with V12CBD and exposed either to macrophage RAW264.7 (F) or to peritoneal macrophages from BALB/c mouse for 4 h (G).  $n = 9$  (F) and  $n = 6$  (G). \*\* $P < 0.01$ , \*\*\* $P < 0.001$ .

H Effect of V12CBD on the virulence of *S. aureus* in vivo. *Staphylococcus aureus* T23 is pre-bound with varied V12CBD (0  $\mu\text{g/ml}$ , black line; 100  $\mu\text{g/ml}$ , green line; 200  $\mu\text{g/ml}$ , red line; 400  $\mu\text{g/ml}$ , blue line) and injected intraperitoneally to mice.  $n = 5$ . \* $P < 0.05$ , \*\*\* $P < 0.001$ .

Data information: Data are expressed as mean  $\pm$  SEM. Pairwise comparison is performed using two-tailed Student's  $t$ -test.

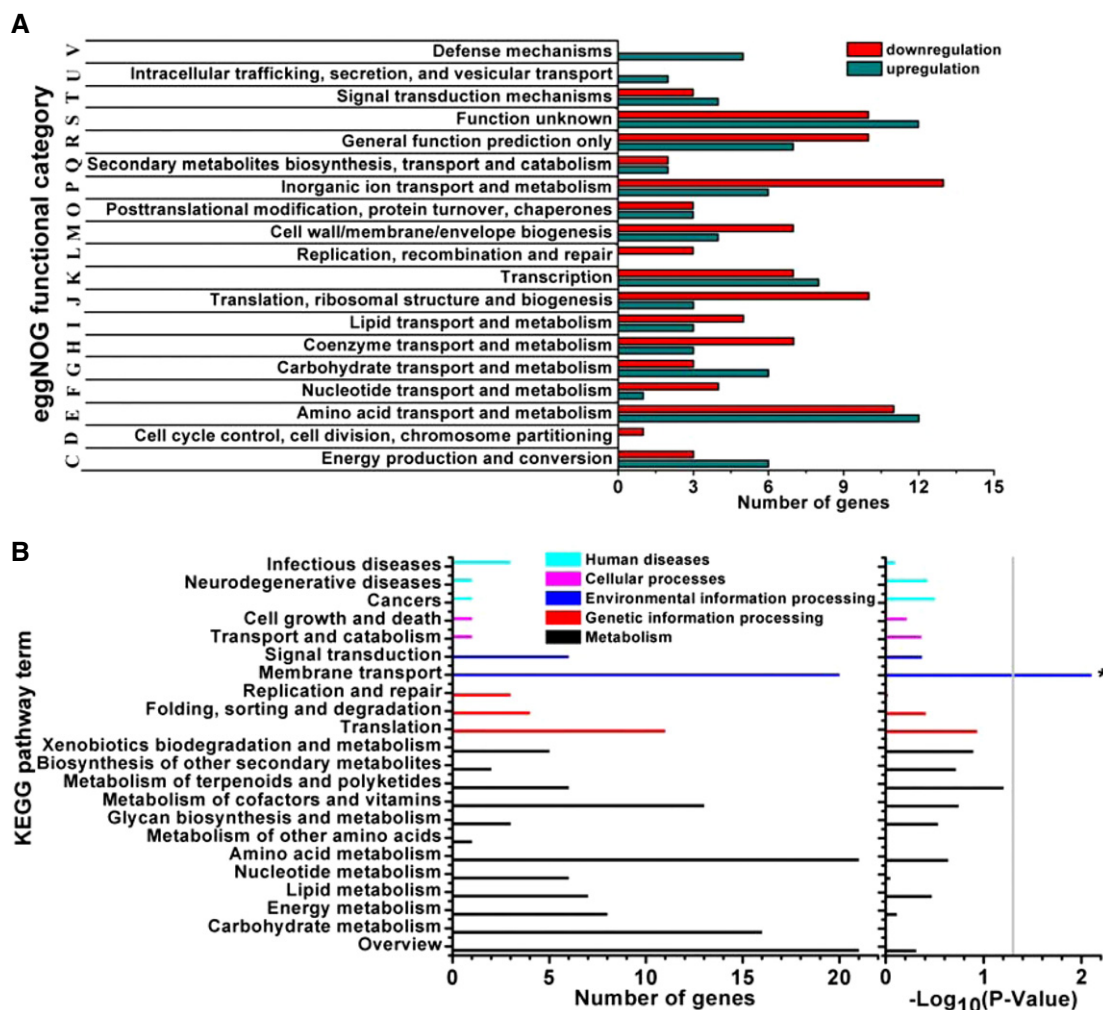
of binding with V12CBD on the transcriptional response of *S. aureus* T23. In summary, a total of 225 differentially expressed genes (DEGs) were identified (at least twofold change, with a  $P$ -value

$< 0.05$ ) after V12CBD treatment (Appendix Table S1). Of those, transcripts of 111 genes were found upregulated and 114 downregulated in response to V12CBD. Predominantly, genes involved in

translation (76.9%), nucleotide metabolism (80%), and cell division (100%), as well as replication and repair (82%), were repressed in *S. aureus* treated with V12CBD (Fig 2A). The GO enrichment analysis showed that the DEGs were scattered in 34 GO terms, specifically, a total of three items related to cellular components, 25 items for biological processes, and six items for molecular functions (Appendix Fig S4). Functional classification of the DEGs using KEGG (Kyoto Encyclopedia of Genes and Genomes) pathway enrichment analysis revealed that a large group of *S. aureus* genes expressed differentially in response to V12CBD belonged to the membrane transport pathway, the environmental information processing category (Fig 2B). Particularly, genes belonging to ABC transports such as *pstA*, *cycB*, *opuA*, *abca/bmrA*, *opuBD*, *msbA*, and *nikC*, genes involved in phosphotransferase system such as *lacE*, as well as genes involved in bacterial secretion system including *secD* and *secY*, were upregulated in *S. aureus* (Appendix Table S1). Because the ABC transports play significant roles in nutrient uptake and in

secretion of toxins and antimicrobial agents in bacteria (Davidson & Chen, 2004), the increased expression of the genes encoding these pathways in the presence of V12CBD indicates a certain degree of nutrient limitation of *S. aureus*. This nutrient limitation may lead to the upregulation of genes that enable *S. aureus* to uptake amino acids (*opuBD*), phosphate ion (*pstA*), lipids (*abca/bmrA*), and sugars (*cycB*) from the extracellular microenvironment. Also, several genes involved in ABC transports such as *modB*, *znuA*, *oppA/mppA*, *phnD*, and *metN* were found downregulated (Appendix Table S1), most of which were substrate-binding proteins in iron complex transport system.

Several genes encoding important virulence factors, such as surface protein-encoding gene *sdrC*, which is a well-characterized surface-associated protein that mediates the adhesion of *S. aureus* to biomaterial and host cell surface (Barbu et al, 2014), protein arginine kinase encoding gene *mcsB*, which is required for stress tolerance and virulence of *S. aureus* (Wozniak et al, 2012), persistent



infection-associated genes (*putP* and *oppF2*), and the genes involved in capsular polysaccharide biosynthesis (*tarI* and SAOUHSC\_00125), were downregulated in the presence of V12CBD (Table 1 and Appendix Table S1). Since most *S. aureus* strains are L-proline auxotrophs, PutP catalyzes the sodium-dependent uptake of extracellular L-proline that contributes to *in vivo* survival and persistent infection of *S. aureus* (Schwan et al, 1998; Bayer et al, 1999). The gene product of *oppF2* is involved in oligopeptide uptake that has been proven important for *S. aureus* growth and survival in multiple infection environments (Coulter et al, 1998). And capsular polysaccharides are important for *S. aureus* to evade the host innate immune defenses (Thakker et al, 1998; Cunnion et al, 2001).

Two of 16 two-component systems (TCSs; Beier & Gross, 2006; Stock et al, 2000) of *S. aureus* (WalKR and SrrAB) were also found downregulated in the presence of V12CBD (Table 1 and Appendix Table S1). The WalKR TCS, originally identified in *Bacillus subtilis* (Fabret & Hoch, 1998), is highly conserved and specific to low G+C Gram-positive bacteria, including *S. aureus* (Martin et al, 1999). The WalKR system is considered as the only essential TCS for the viability of *S. aureus* and plays a central role in controlling cell wall metabolism, oxidative stress resistance, and virulence regulation (Dubrac et al, 2007; Ji et al, 2016). The *walKR* operon of *S. aureus* comprises five-jointed gene locus, that is, *walR*, *walK*, *yycH*, *yycI*, and *yycJ*, under a Sigma A-dependent promoter (Dubrac et al, 2008). Although the genes encoding *yycI* and *yycJ* were not DEGs, the expression levels of *walR* and *yycH* were greatly repressed in V12CBD-treated *S. aureus* (Table 1 and Appendix Table S1). The reduced expression of *walR* indicates reduced virulence, since *walR* positively regulates the expression of major virulence genes involved in host matrix interactions, cytolysis, and host inflammatory response (Delaune et al, 2012). SrrAB (staphylococcal respiratory response AB) is another well-known TCS of *S. aureus* that helps survival of *S. aureus* (Kinkel et al, 2013) and protects *S. aureus* from neutrophil killing in low-oxygen conditions (Ulrich et al, 2007). The repressed expression of *srrAB* system may lead to reduced *ica* gene transcription and polysaccharide intercellular adhesion expression in *S. aureus* (Ulrich et al, 2007), which also imply reduced virulence.

Furthermore, to confirm the effect of V12CBD on the expression of virulence factors of *S. aureus*, the RNA-Seq results were validated

by quantitative real-time PCR (qRT-PCR). In general, there was a positive correlation between the data obtained from qRT-PCR and that from the Illumina RNA-Seq (Table 1). Interestingly, the expression level of *walR* in *S. aureus* was strikingly declined (fold change from  $-3.35$  to  $-93.05$ ) when V12CBD concentration increased from 25 to 100  $\mu\text{g/ml}$  (Table 1), indicating that the WalKR TCS may be the main system that senses the change of V12CBD in the environment.

### V12CBD enhances phagocytosis and killing of *Staphylococcus aureus* by macrophages

In order to minimize the possible effects of residual V12CBD on the RAW264.7 cells in the above experiments, we examined the phagocytic capacity of V12CBD-treated macrophages against WGA-conjugated *S. aureus* N315 by flow cytometry (Fig 3A). Unexpectedly, treatment with V12CBD indicated substantial phagocytosis of *S. aureus* by macrophage RAW264.7 in a dose-dependent manner (Fig 3B). After treatment with 100  $\mu\text{g/ml}$  V12CBD, phagocytosis of staphylococci increased about 2.9-fold (47.6% vs. 16.5%). Accordingly, the survival rates of *S. aureus* in the macrophages declined along with the increase in the treatment concentration of V12CBD (Fig 3C). Additional experiments showed that V12CBD (labeled with Alexa Fluor 488) could not permeate A549 cells (Appendix Fig S5), but can be taken up by the macrophages in a time-dependent manner (Fig 3D and Appendix Fig S5).

Because the innate immune system provides the first line of defense to the host by initiating a sequence of events that result in the production and secretion of a wide range of inflammatory cytokines, the activation of macrophages, and the initiation of adaptive immunity (Fournier & Philpott, 2005), in order to further understand the mechanisms behind the finding that V12CBD can enhance phagocytosis and killing of *S. aureus* by macrophages (Fig 3A–C), we examined the effects of V12CBD on the expression of several cytokines of macrophage by qRT-PCR. Because V12CBD was expressed by *Escherichia coli*, to exclude the possible effects of contaminated LPS, we detected the expressions of these genes in the presence of LPS inhibitor polymyxin B. It was found that polymyxin B could completely block the stimulation effect of LPS (Appendix Fig S6A), but not the effects of V12CBD on the gene

**Table 1. Virulence-associated DEGs expressed by *Staphylococcus aureus* in the presence of V12CBD.**

Locus	Gene	Description	Fold change	
			RNA-Seq	qRT-PCR
SAOUHSC_00544	<i>sdrC</i>	Serine-aspartate repeat-containing protein C	-2.42	-2.71 (-23.4)
SAOUHSC_00125		Cap5L protein/glycosyltransferase	-3.25	-3.57 (-12.42)
SAOUHSC_00225	<i>tarI</i>	Ribitol-5-phosphate cytidyllyltransferase 1	-4	-9.43 (-7.55)
SAOUHSC_00504	<i>mcsB</i>	Protein arginine kinase	-3	-5.61 (-5.36)
SAOUHSC_02119	<i>putP</i>	Sodium/proline symporter	-3.93	-4.22 (-3.01)
SAOUHSC_01377	<i>oppF2</i>	Putative oligopeptide transport ATP-binding protein	-2.62	-
SAOUHSC_00020	<i>walR</i>	Transcriptional regulatory protein	-2.45	-3.35 (-93.05)
SAOUHSC_01586	<i>srrA</i>	Transcriptional regulatory protein	-3.83	-

DEGs, differentially expressed genes.

The fold changes in qRT-PCR represent the expression levels of *S. aureus* in the presence of 25 and 100  $\mu\text{g/ml}$  V12CBD, respectively.

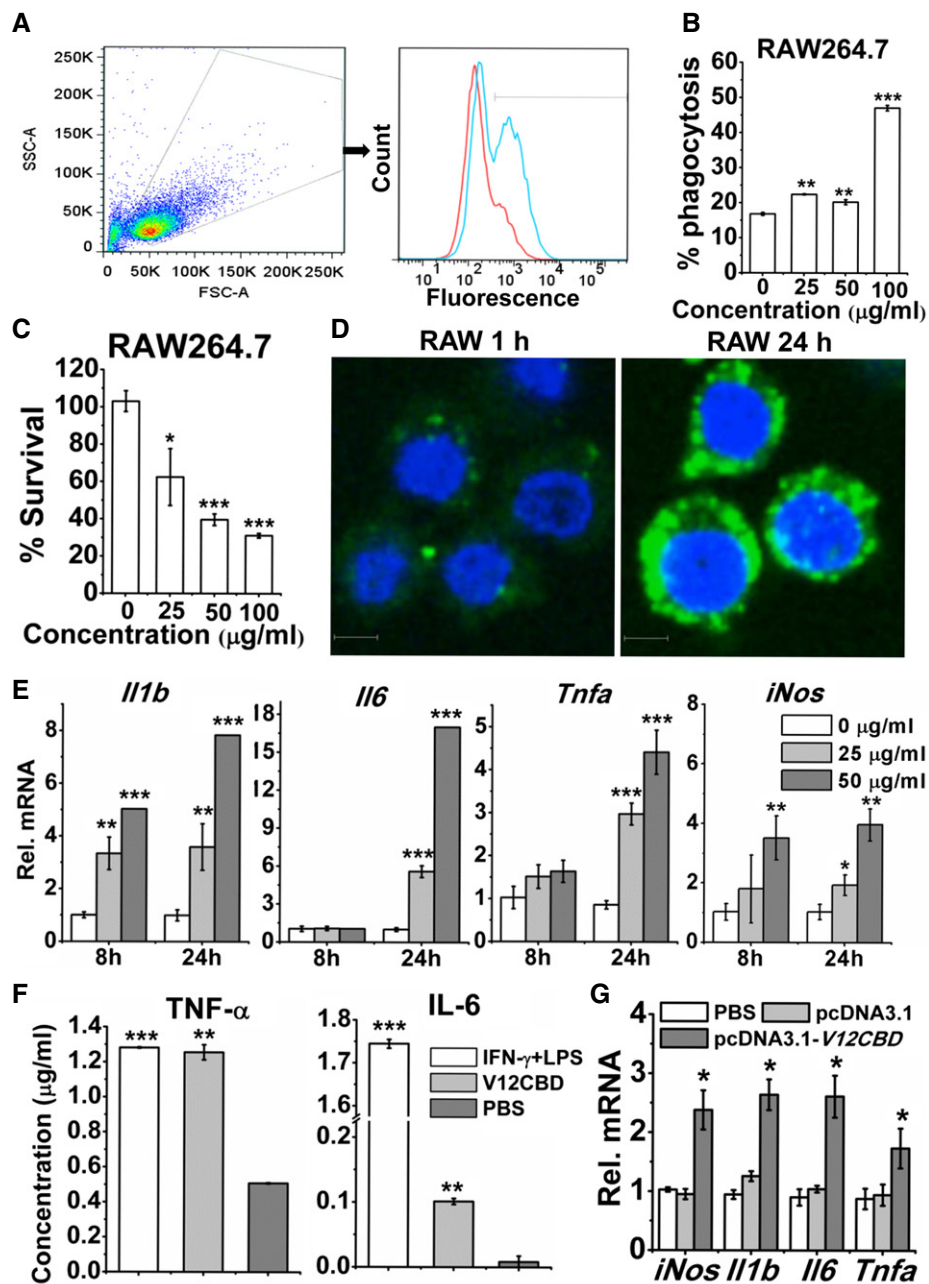


**Figure 3. V12CBD activates macrophages and promotes their phagocytosis and killing against *Staphylococcus aureus*.**

A Example FACS plot for phagocytosis of *S. aureus* by V12CBD-pretreated macrophages. RAW264.7 cells are pretreated with V12CBD (cyan line) or PBS (red line) for 24 h before the experiment. Then, WGA-conjugated *S. aureus* N315 is added and cocultured with RAW264.7 cells for 1 h. After treatment with trypsin and washing with PBS at 300 g for six times, RAW264.7 cells are analyzed using a BD LSRFortessa flow cytometer. Images shown are representative of two independent repeats ( $n = 3$  per group).

B Summary data of phagocytosis of *S. aureus* by macrophages. The extent of phagocytosis after each treatment is analyzed using the CFlow software.  $n = 6$ .  $^{**}P < 0.01$ ,  $^{***}P < 0.001$ .

C Survival of *S. aureus* in RAW264.7 cells pretreated with V12CBD for 24 h.  $n = 6$ .  $^{*}P < 0.05$ ,  $^{***}P < 0.001$ .

D Images of RAW264.7 cells after cocultured with Alexa Fluor 488-labeled V12CBD for 1 and 24 h. Scale bar: 5  $\mu\text{m}$ . Images shown are representative of two independent repeats ( $n = 3$  per group).

E Expression levels of *Il1b*, *Il6*, *Tnfa*, and *iNos* in macrophage RAW264.7 after exposure to 0, 25, and 50  $\mu\text{g/ml}$  V12CBD for 8 and 24 h.  $n = 6$ .  $^{*}P < 0.05$ ,  $^{**}P < 0.01$ ,  $^{***}P < 0.001$ .

F Expression levels of TNF- $\alpha$  and IL-6 in the supernatants of RAW264.7 after treated with 100  $\mu\text{g/ml}$  V12CBD for 24 h. Cells treated with a mixture of 15 ng/ml IFN- $\gamma$  and 15 ng/ml LPS are used as positive controls.  $n = 3$ .  $^{**}P < 0.01$ ,  $^{***}P < 0.001$ .

G Expression levels of *Il1b*, *Il6*, *Tnfa*, and *iNos* in BHK-21 cells after transfection with pcDNA3.1 or pcDNA3.1-V12CBD for 48 h.  $n = 6$ .  $^{*}P < 0.05$ .

Data information: Data are shown as mean  $\pm$  SEM. Pairwise comparison is performed using two-tailed Student's *t*-test, unless stated otherwise. All genes' expression levels are compared with that of *Gadph* gene in the same condition. The PBS-treated cells were used as blank controls.

expression profiles of macrophage (Appendix Fig S6B). Further results showed that the expression of genes encoding a core set of proinflammatory cytokines, i.e., interleukin-1 $\beta$  (IL-1 $\beta$ ), IL-6, and tumor necrosis factor alpha (TNF- $\alpha$ ), as well as inducible nitric oxide synthase (iNOS), was upregulated in V12CBD dose-dependent manners after treating macrophage RAW264.7 with V12CBD for 24 h (Fig 3E), while the expression of the gene encoding Toll-like receptor 4 (TLR4, the receptor of LPS) did not have significant changes (Appendix Fig S7). Correspondingly, increased accumulations of TNF- $\alpha$  (from 0.51 to 1.25  $\mu$ g/ml) and IL-6 (from 0.0084 to 0.10  $\mu$ g/ml) were detected by ELISA in supernatants of RAW264.7 cells treated with V12CBD for 24 h in comparison with that of the PBS-treated wells (Fig 3F). The increased expressions of genes encoding TNF- $\alpha$ , IL-1 $\beta$ , IL-6, and iNOS reveal a classically activated status of macrophages that is typical for clearing primary infections (Serbina *et al*, 2003). More interesting, much higher expression of the gene encoding iNOS was observed after coculturing V12CBD-treated macrophages with *S. aureus* for 2 h (Appendix Fig S8), which may be part of the reasons for decreased survival of *S. aureus* observed in Fig 3C. Increased expressions of genes encoding IL-1 $\beta$ , IL-6, or TNF- $\alpha$  were also observed in V12CBD-treated macrophages after coculture with *S. aureus* for 4 and 8 h (Appendix Fig S8). However, decreased expressions of genes encoding IL-1 $\beta$  and TNF- $\alpha$  were observed in V12CBD-treated macrophage after coculture with *S. aureus* for 24 h (Appendix Fig S8), suggesting that V12CBD-treated macrophages might have an alleviated inflammation after 24 h of *S. aureus* infection.

To further confirm the effects of V12CBD on the expressions of inflammatory cytokines, we cloned V12CBD coding sequence into plasmid pcDNA3.1 and transfected the expression vector (pcDNA3.1-V12CBD) into non-phagocytic BHK-21 cells. Results showed that similar increased expressions of genes encoding TNF- $\alpha$ , IL-1 $\beta$ , IL-6, and iNOS are observed in cells after transfection with pcDNA3.1-V12CBD for 48 h in comparison with cells transfected with pcDNA3.1 vector alone (Fig 3G).

### V12CBD activates macrophages through NF- $\kappa$ B pathway

Since classically activated macrophages are able to express specific marker molecules, such as CC chemokine receptor 7 (CCR7), efficient antigen-presenting molecules, such as MHC class II (MHCII), and costimulatory molecules, such as CD80 and CD86 on surface (Mosser & Edwards, 2008), we further determined the expression levels of these molecules in macrophages after exposure to V12CBD for 24 h. An increased expression of CCR7 (from 1.15 to 5.8%), CD80 (from 77.15 to 84%), and MHCII (from 1.05 to 6.05%) was detected in the macrophages by antibody-specific flow cytometry (Fig 4A–D). These results indicate that V12CBD promotes the classical activation of macrophages.

It is well known that MAPSs and NF- $\kappa$ B signaling pathways are involved in macrophage activation (Mosser & Edwards, 2008). Our further study using signal blocking assays and qRT-PCR method showed that upregulations of both genes encoding IL-6 and iNOS evoked by V12CBD are significantly depressed after inhibiting NF- $\kappa$ B pathway with BAY 11-7082 (Fig 4E), suggesting that just NF- $\kappa$ B pathway, but not MAPK pathways, plays a critical role in the activation of macrophages by V12CBD. Moreover, *in situ* detection of phospho-NF- $\kappa$ B-p65

protein by flow cytometry showed that an obvious upregulation is occurred in macrophages treated with V12CBD for 15 min compared with that of the PBS-treated control (Fig 4F). The time-dependent analysis also showed that the expression of phospho-NF- $\kappa$ B-p65 protein is increased 2.96-fold after treating the macrophages with 100  $\mu$ g/ml V12CBD for 30 min (Fig 4G).

### V12CBD is a therapeutic and prophylactic agent against MRSA infection in mice

As V12CBD sensitizes *S. aureus* to immune clearance (Fig 1F–H) and represses multiple virulence genes expression (Table 1), we next sought to determine the therapeutic efficacy of V12CBD on a *S. aureus* sepsis model. We infected mice with a lethal dose of MRSA T23 intraperitoneally ( $2.5 \times 10^8$  CFU/mouse). Three hours post-infection, mice were received a single intraperitoneal injection of V12CBD. As shown in Fig 5A and B, treatment with V12CBD improved the survival time of the MRSA-infected mice in a dose-dependent manner, and a survival rate of 60% (6/10) at day 10 after infection was observed in mice administrated with 12 mg/kg V12CBD, whereas the PBS-treated mice ( $n = 6$ ) died within 1 day after the infection.

As V12CBD activates macrophages (Fig 3), the preventive efficiency of V12CBD against MRSA infection was also tested in the mouse model of sepsis. Each mouse was received a single intraperitoneal injection of 12 mg/kg V12CBD or an equal volume of PBS. Twenty-four hours later, the mice were challenged intraperitoneally with a lethal dose of  $2 \times 10^8$  CFU/mouse of MRSA T23 (Fig 5C). Mouse viability was monitored for 10 days, at which time surviving mice were euthanized. The survival of V12CBD-treated mice was significantly improved compared with that of the control mice (81.25% vs. 10%, Fig 5D).

To evaluate the cytotoxicity of V12CBD, we examined the viability of Caco-2 and CHO cells exposed to V12CBD by CCK-8 assay. No obvious cytotoxicity was observed in both cell lines even at a concentration of 1,000  $\mu$ g/ml (Appendix Fig S9). Moreover, a single dose of 1 mg/mouse V12CBD did not show any harmful effects on mortality and viability of the experimental animals in a 10-day observation course (Appendix Fig S10). These results imply that V12CBD would be safe for *in vivo* applications.

### Preventive administration of V12CBD reduces bacterial loads in organs

To further examine the prophylactic effect of V12CBD in blocking the virulence of *S. aureus*, we firstly treated female BALB/c mice with PBS ( $n = 7$ ) or 12 mg/kg V12CBD ( $n = 8$ ) intraperitoneally. Twenty-four hours later, the mice were challenged intraperitoneally with a sublethal dose of  $1.3 \times 10^8$  CFU of MRSA T23. Three days later, surviving mice were euthanized, the proinflammatory cytokines in blood and pathological changes in organs were monitored, and the bacterial loads in organs were determined through homogenization, serial dilution, and plating (Fig 6A). Treatment with V12CBD significantly decreased the staphylococcal loads in both livers ( $\sim 2.54 \log_{10}$  cfu/organ reduction) and kidneys ( $\sim 1.64 \log_{10}$  cfu/organ reduction; Fig 6B). Specifically, the *S. aureus* loads in two of the V12CBD-treated mice (2/8) reduced to that below the limit of detection (no bacteria was detected in 10  $\mu$ l of the 1 ml

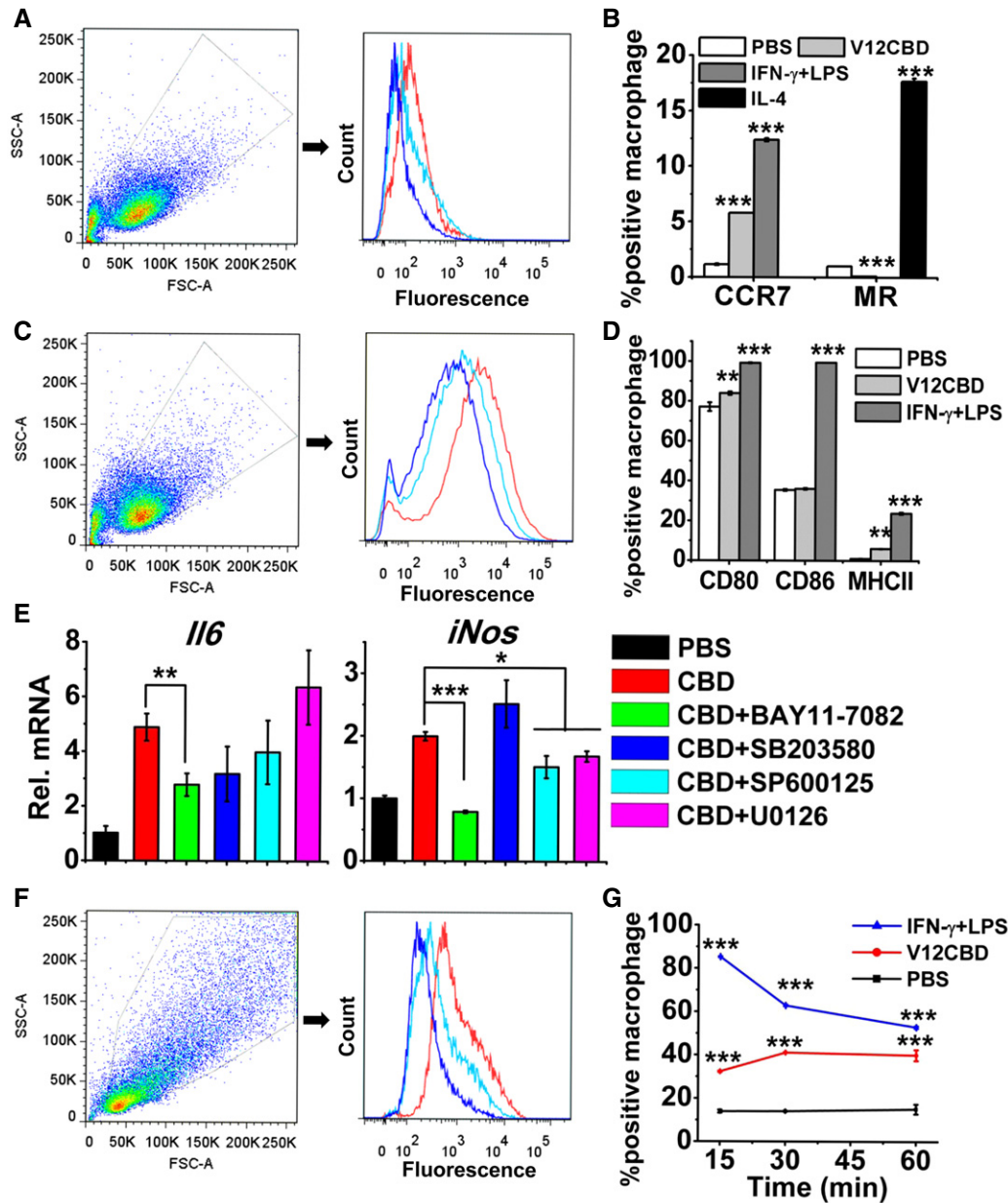


**Figure 4. V12CBD activates NF- $\kappa$ B pathway in macrophages.**

A Example FACS plot for the detection of CCR7 in macrophages (red line: IFN- $\gamma$  + LPS; cyan line: V12CBD; and blue line: PBS). Images shown are representative of two independent repeats ( $n = 3$  per group).

B Summary data of CCR7 and MR levels in macrophage after treated with 50  $\mu$ g/ml V12CBD for 24 h. Cells treated with 20 ng/ml IL-4 and a mixture of 15 ng/ml IFN- $\gamma$  and 15 ng/ml LPS are used as the positive control for MR and CCR7 detection, respectively.  $n = 6$ . \*\*\* $P < 0.001$ .

C Example FACS plot for the detection of CD80 in macrophages (Red line: IFN- $\gamma$  + LPS; Cyan line: V12CBD; and Blue line: PBS). Images shown are representative of two independent repeats ( $n = 3$  per group).

D Summary data of CD80, CD86, and MHCII levels in macrophage after treated with 50  $\mu$ g/ml V12CBD for 24 h.  $n = 6$ . \*\* $P < 0.01$ , \*\*\* $P < 0.001$ .

E Effects of various signaling inhibitors on the expression of *Il6* and *iNos* in macrophage after exposure to V12CBD. RAW264.7 cells are pretreated with different signaling inhibitors (BAY 11-7082, targeting NF- $\kappa$ B pathway; SB203580, targeting p38MAPK pathway; SP600125, targeting JNK pathway; or U012, targeting ERK1/2 pathway) for 30 min, washed, and cocultured with 50  $\mu$ g/ml V12CBD for 24 h before qRT-PCR analysis. All genes expression levels are compared with that of *Gadph* gene in the same condition.  $n = 3$ . \* $P < 0.05$ , \*\* $P < 0.01$ , \*\*\* $P < 0.001$ .

F Example FACS plot for the detection of phospho-NF- $\kappa$ B-p65 in macrophages after treated with V12CBD for 15 min (Red line: IFN- $\gamma$  + LPS; Cyan line: V12CBD; and Blue line: PBS). RAW264.7 cells are treated with 100  $\mu$ g/ml V12CBD for 15, 30, and 60 min, respectively. After fixation and staining with specific antibody, macrophages are analyzed by flow cytometry. Images shown are representative of two independent repeats ( $n = 3$  per group).

G Summary data of phospho-NF- $\kappa$ B-p65 level in macrophage in time course. The ratio of fluorescent macrophages in each treatment is calculated using the CFlow software.  $n = 6$ . \*\*\* $P < 0.001$ .

Data information: Data are expressed as mean  $\pm$  SEM. Pairwise comparison is performed using two-tailed Student's  $t$ -test.



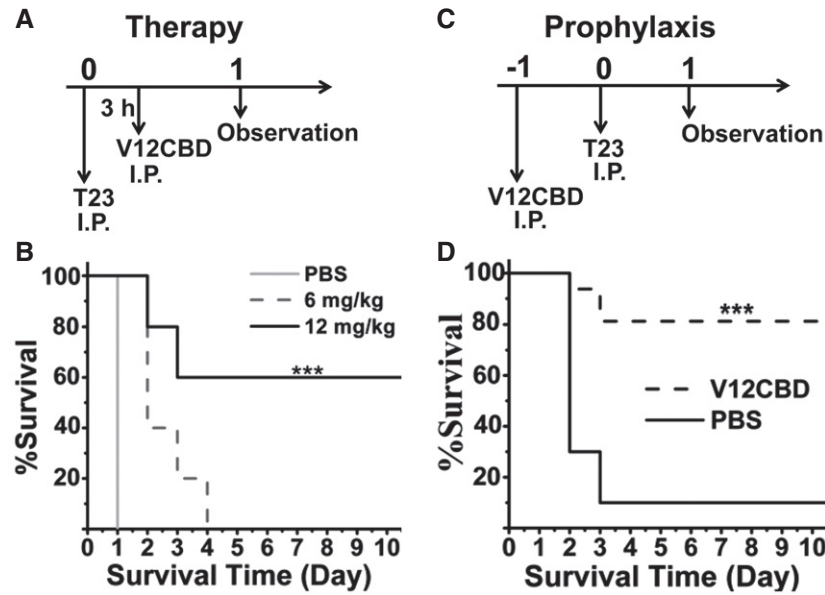


**Figure 5. Protective efficacy of V12CBD in MRSA-infected mouse models.**

- A Schematic of the MRSA-infected therapeutic model.
- B Therapeutic efficacy of V12CBD in MRSA-infected therapeutic model. Mice are infected intraperitoneally with a lethal dose of  $2.5 \times 10^8$  CFU of *S. aureus* T23 and then received a single dose of 6 mg/kg ( $n = 10$ ), or 12 mg/kg V12CBD ( $n = 10$ ), or equal volumes of PBS ( $n = 6$ ) at 3 h post-infection.  $***P < 0.001$ .
- C Schematic of the MRSA-infected prophylactic model.
- D Preventive efficacy of V12CBD in MRSA-infected prophylactic model. Mice are received intraperitoneal injection at a single dose of 12 mg/kg V12CBD ( $n = 14$ ) or equal volumes of PBS ( $n = 10$ ). Twenty-four hours later, mice are received a lethal dose of  $2 \times 10^8$  CFU of *S. aureus* T23. The mortality and the weight of each group are recorded for 10 days.  $***P < 0.001$ .

Data information: Survival analysis is analyzed using log-rank test.

homogenized organ suspension). While in the PBS-treated control group, one mouse died at day 3. The health scores of the V12CBD-treated mice were significantly improved compared to that of the PBS-treated control mice (Fig 6C). Meanwhile, a reduced weight loss was detected in the V12CBD-treated mice (average weight loss of 10.8% vs. 20.6% in the control group, Appendix Fig S11). In addition, treatment with V12CBD significantly reduced the level of TNF- $\alpha$  (~ 11.5-fold reduction at day 3) in the sera (Fig 6D), a main proinflammatory cytokine that involves in the induction of *S. aureus*-associated sepsis shock (Verhoef & Mattsson, 1995). Accordingly, less inflammatory injury in organs caused by *S. aureus* sepsis was observed in the V12CBD-treated mice. Alleviated injury could be seen in the tissue sections of V12CBD-treated mice (Appendix Fig S12), especially kidney and liver tissues, showing reduced interstitial inflammatory cell infiltration and dilation, and ameliorated histopathological changes by comparison with that of PBS-treated controls. These results showed that preventive administration of V12CBD could accelerate the clearance of *S. aureus* *in vivo* and reduce inflammation and related immune injury evoked by *S. aureus* infection.

We next examined whether the preventive effect of V12CBD against *S. aureus* infection was strain-specific. Another MRSA strain N315 was tested in the mouse model of sepsis, to measure bacteria survival in the host organs. *S. aureus* strain N315 is a hospital-acquired MRSA strain isolated in Japan (Ito et al., 1999). As expected, similar results were observed as to that of *S. aureus* T23 infection. First, the heavy weight loss due to *S. aureus* N315

infection was reduced in V12CBD pretreated mice (Fig 6E). Second, V12CBD caused a  $> 0.95 \log_{10}$  cfu/organ reduction in staphylococcal loads in livers and a  $> 1.09 \log_{10}$  cfu/organ reduction in kidneys (Fig 6F). To our surprise, treatment with V12CBD also resulted in reduction in bacterial loads in the hearts (~ 0.92  $\log_{10}$  cfu/organ reduction) and the spleens (~ 1.07  $\log_{10}$  cfu/organ reduction) of the infected mice, although the decrease was not significant (Fig 6F).

## Discussion

The emerging of MDR pathogens and the lagging of new antibiotic development make it urgent to develop new anti-infective approaches. In the present study, we found, for the first time, that a protein, V12CBD, derived from the cell wall binding domain of bacteriophage lysin PlyV12 has multiple functions, not only attenuating *S. aureus* virulence factors, but also sensitizing them to immune clearance. These unique functions would render V12CBD a novel molecule to control MDR *S. aureus* infections as an alternative to antibiotics.

Lysins are highly evolved molecules that have involved in the coevolution between bacteria and their phages over a billion years (Pastagia et al., 2013). The binding domain of lysins (CBDs) can recognize the conserved wall carbohydrates of target pathogens which have rare chances to evade such recognition (Pastagia et al., 2013). No resistance to lysins is observed after repeated induction in

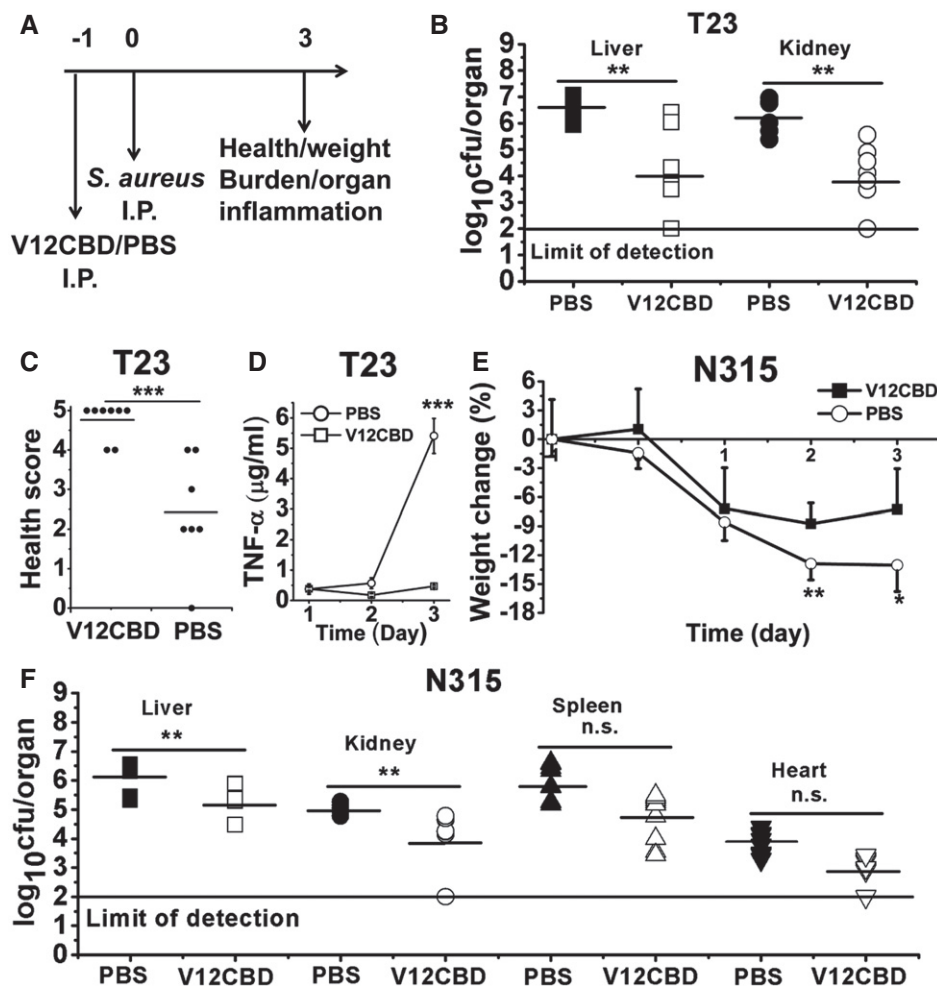


**Figure 6. Preventive administration of V12CBD reduces *Staphylococcus aureus* loads in infected mouse organs.**

**A** Schematic of the MRSA-infected prophylactic model.

**B, C** Bacterial burden (**B**) and health score (**C**) of the infected mice on day 3. Each symbol represents the value for an individual mouse. Horizontal bars indicate the means of observation, and the solid line marks limit of detection. PBS group:  $n = 7$ ; V12CBD group:  $n = 8$ . \*\* $P < 0.01$ , \*\*\* $P < 0.001$ .

**D** The levels of TNF- $\alpha$  cytokine in mice sera post-infection.  $n = 5$ . \*\*\* $P < 0.001$ .

**E** Weight loss of mice infected with *S. aureus* N315 during the experiment.  $n = 10$ . \* $P < 0.05$ , \*\* $P < 0.01$ .

**F** Effect of V12CBD on *S. aureus* N315 survival in the organs of mice. Each symbol represents the value of an individual mouse. Horizontal bars indicate the means of observation, and the solid line represents the limit of detection.  $n = 10$ . \*\* $P < 0.01$ , n.s., not significant.

Data information: Data are expressed as mean  $\pm$  SEM. Pairwise comparison was performed using two-tailed Student's  $t$ -test.

experimental conditions that readily produce antibiotic resistance (Loeffler *et al*, 2001; Schuch *et al*, 2002). Furthermore, binding with CBD does not kill the bacteria directly, which poses less selective pressure on the pathogen. These properties would mean that few *S. aureus* strains would evolve to be resistant to V12CBD, not like antibiotics.

One significant advantage of V12CBD-based therapy over the whole lysin therapy is sensitization of pathogen to clearance by host innate immune defense, but not cell lysis. Lysin therapy, which is depicted by robust and efficient killing of target bacteria, has been pursued as a promising alternative therapeutic in the latest decades (Nelson *et al*, 2012; Pastagia *et al*, 2013). However, for *S. aureus*, lysin-mediated cell lysis will give rise to the release of a large amount of intracellular enterotoxins, toxic shock

syndrome toxins, cell wall associated and secreted proteins, nucleic acids, and proteases to sites of infection and inflammation, which will evoke harmful immune response of the host and even lead to cytokine storm and shocks (Foster, 2005; Veldkamp & van Strijp, 2009). In these contents, V12CBD could overcome these shortcomings of lysins *via* multiple ways (Fig 7). In one hand, binding with V12CBD can sensitize *S. aureus* to immune clearance characterized by reduced adhesion and invasion to epithelial cells and increased susceptibility to macrophages in comparison with that of native bacteria (Fig 1). The reduced internalization of *S. aureus* after binding with V12CBD (Fig 1B) may be due to the reduced adhesion caused by V12CBD (Fig 1A). In another hand, binding with V12CBD can sensitize *S. aureus* to immune clearance by inhibiting specific virulence factors essential for the pathogen's survival

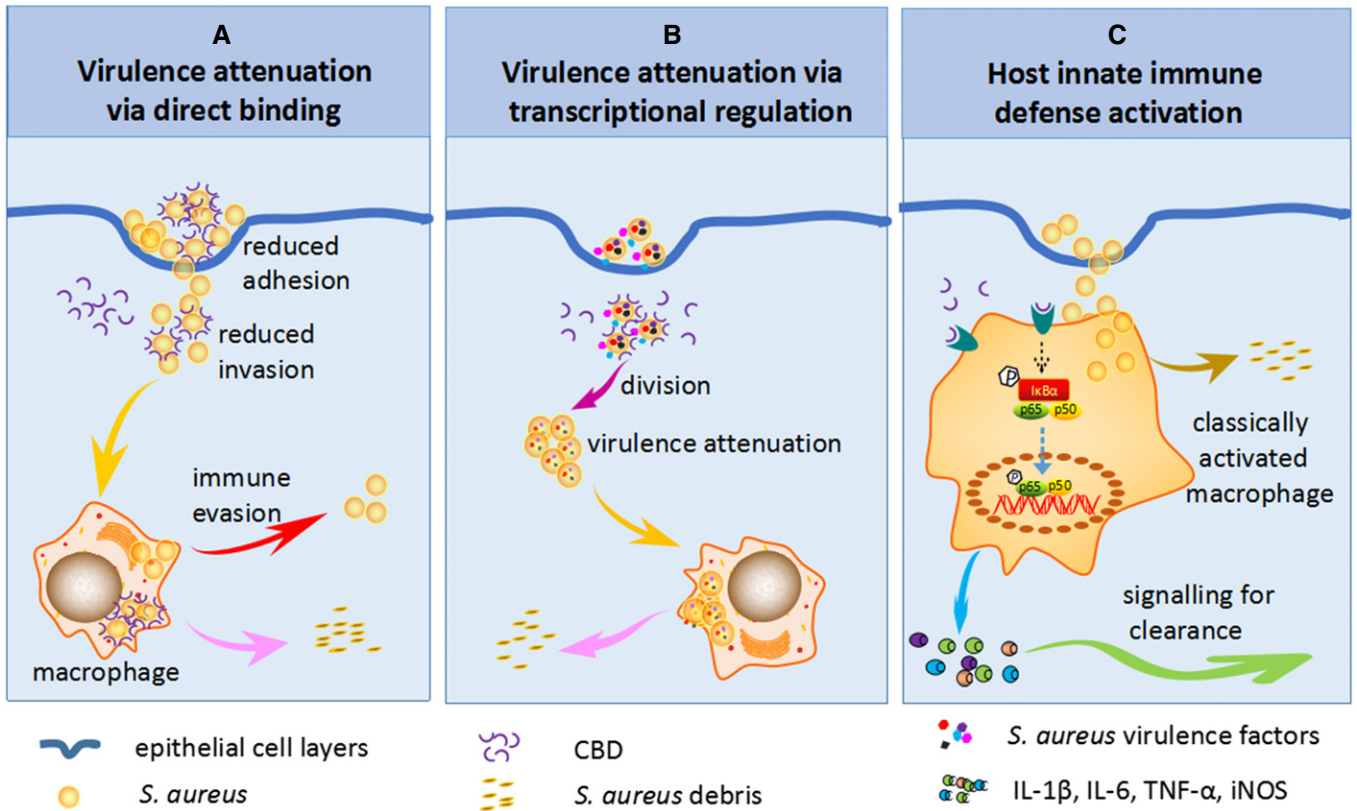


**Figure 7. Schematic of the working models of V12CBD.**

A–C V12CBD can sensitize *Staphylococcus aureus* to immune clearance via direct binding to bacterial cell surface (A), suppress the expression of multiple virulence factors of *S. aureus* (B), and enhance host innate immunity through NF- $\kappa$ B pathway-mediated macrophage activation (C).

during infection (Fig 2), such as *sdrC*, *traI*, and the gene (SAOUHSC\_00125) involved in capsular polysaccharide biosynthesis, and *mcsB*, *putP*, and *oppF2* that help *S. aureus* survival and persistence in hosts.

Another significant merit of V12CBD would be that it can be applied not only as a therapeutic anti-infective, but also as prophylaxis to prevent *S. aureus* infection. This unique property has not been reported before. We observed that V12CBD stimulated the phagocytosis and killing of *S. aureus* in dose-dependent manners (Fig 3). Initial data showed that V12CBD promoted the classical activation of macrophages via NF- $\kappa$ B pathway (Fig 4). Increased expressions of genes encoding IL-1 $\beta$ , IL-6, TNF- $\alpha$ , and iNOS would play multiple functions to mediate host immune defense against pathogens, including the activation of T cells (IL-1 $\beta$ ) and phagocytes (TNF- $\alpha$ ), stimulation of terminal differentiation and immunoglobulin secretion (IL-6) of B cells, and production of reactive nitrogen intermediates (iNOS; Fournier & Philpott, 2005). It is well known that the production of reactive nitrogen intermediates by iNOS comprises one of the major mechanisms in host innate immune system for killing invaded pathogens (Aktan, 2004). Although these results suggest that V12CBD could activate macrophages via NF- $\kappa$ B pathway, the detailed mechanism underlying the activation needs further study. At the same time, it is possible that, as a positively charged protein, V12CBD (pI = 9.96) might non-specifically bind with negatively charged molecules in *E. coli* lysate and *in vivo*, which might

affect the function of V12CBD. Since no cytotoxicity was observed for V12CBD at cell and animal levels, there is a great possibility that preventive administration of V12CBD could be used to alleviate host inflammation and immune injury caused by staphylococcal infection.

Last but not least, as a foreign protein, V12CBD may elicit specific antibodies after injection, which might neutralize the protection efficacy of V12CBD. However, previous studies have showed that lysin-specific antibodies could not neutralize their bacteriocidal activity (Pastagia *et al*, 2013), which relies on the binding of CBDs to wall carbohydrates of target bacteria and digestion of the peptidoglycan bonds by catalytic domains. Based on these results, it is probably that the antibodies elicited by V12CBD could not neutralize its binding activity.

In conclusion, this study found for the first time that the lysin-derived V12CBD is a multifunctional molecule (Fig 7). On one hand, it can interplay with *S. aureus* to attenuate the virulence and increase their susceptibility to host immune clearance; on the other hand, it can interact with host via activating phagocytes (i.e., macrophages) to accelerate the clearance of invaded pathogens. In view of good therapeutic and preventive efficiency of V12CBD, the lysin-derived protein would represent a novel anti-infective against antibiotic-resistant *S. aureus*. More broadly, this anti-infective strategy might be translated to other Gram-positive pathogens, given the wide availability of phage lysins in nature.

## Materials and Methods

Detailed methods can be found in the Appendix Supplementary Methods available online.

### Ethical statement

All mouse experiments were conducted in an ABSL-2 laboratory with the approval of the Animal Experiments Committee of Wuhan Institute of Virology, Chinese Academy of Sciences (approval No. WIVA17201602). Animals were randomized and cared in individually ventilated cages following a set of animal welfare and ethical criteria during the experiments and euthanized at the end of observation.

### Bacterial and cell culture conditions

Methicillin-resistant *S. aureus* strains (N315 PMID: 11418146 and T23) used in this study were cultured in tryptic soy broth (TSB) at 37°C. V12CBD protein was expressed in *E. coli* and purified using affinity chromatography. A549 cells were cultured in Dulbecco's modified Eagle's medium: Nutrient Mixture F-12 (DMEM/F12, Gibco) supplemented with 10% fetal bovine serum (FBS, Sigma-Aldrich), BHK-21 cells, RAW264.7, and peritoneal macrophages were cultured in DMEM supplemented with 10% FBS. Caco-2 cells were grown in DMEM supplemented with 15% FBS, 1% penicillin, and 1% streptomycin. CHO cells were grown in DMEM supplemented with 10% FBS, 1% penicillin, and 1% streptomycin. All cells were cultured in a humidified atmosphere of 5% CO<sub>2</sub> at 37°C.

### Bacterial adhesion and internalization by epithelial cells

Bacterial cells, including *S. aureus* N315, *L. monocytogenes* ATCC 19115 (*Lmo*), *S. agalactiae* S12 (*Sag*), and *S. enteritidis* ATCC 14028 (*Sen*), were pretreated with various concentrations of V12CBD for 1 h, washed with PBS to remove unbound V12CBD, and cocultured with A549 cell at a multiplicity of infection (MOI) of ~ 50 bacterial cells per one epithelial cell for 1 h. After washing with PBS, cell suspension was serially diluted and plated on agar plates to enumerate the total bacteria in each well ( $N_t$ ). The number of internalized bacteria ( $N_i$ ) was determined by enumerating residual viable bacteria after treatment with 200 µg/ml gentamycin for 2 h to kill the bacteria adhered on the cell surface. The bacteria adhered on the cell surface ( $N_a$ ) was expressed as the difference between the total bacteria and internalized ones ( $N_a = N_t - N_i$ ).

### Macrophage killing assay

To assess the killing capacity of naïve macrophage, *S. aureus* N315 was pretreated with various concentrations of V12CBD at 37°C for 1 h, washed by PBS, and cocultured with RAW264.7 or BALB/c peritoneal macrophage cells (MOI ~ 1) for 4 h at 37°C. To test the killing capacity of V12CBD-treated macrophage, RAW264.7 cells were pretreated with various concentrations of V12CBD for 24 h, washed with PBS, and then cocultured with log phase *S. aureus* N315 at 37°C for 4 h. The viable *S. aureus* was determined by plating serial dilutions on TSA agar.

### Macrophage phagocytosis

To assess the phagocytosis capacity of naïve macrophage and V12CBD-treated macrophage, *S. aureus* N315 was labeled with Alexa Fluor 594-conjugated wheat germ agglutinin (WGA, Life Technology) and cocultured with V12CBD pretreated or non-pretreated RAW264.7 cells for 1 h at 37°C. After incubating, wells were washed with PBS to remove extracellular bacteria, and then, cell suspensions were transferred to U-bottomed tubes for flow cytometry analysis (BD LSRFortessa).

### Detection of surface molecules expressed by macrophages

RAW264.7 cells were pretreated with various concentrations of V12CBD for 24 h, washed with PBS, and then labeled with different target-specific antibodies. The expression levels of various surface molecules, including CCR7, MR, CD80, CD86, and MHCII, by macrophages, were analyzed by the LSRFortessa analyzer cytometer (BD).

### In situ detection of phospho-NF-κB-p65 in macrophages

RAW264.7 cells were treated with 100 µg/ml V12CBD, a mixture of 15 ng/ml IFN-γ and 15 ng/ml LPS (positive control), or PBS for different times. After washing with PBS, cells were fixed by 4% paraformaldehyde, permeabilized with 90% methanol, and incubated with rabbit anti-phospho-NF-κB-p65-Ser536 antibody (Invitrogen, Life technology) at room temperature for 60 min. After incubation with an Alexa Fluor 488-conjugated goat anti-rabbit secondary antibody, cells were analyzed by the LSRFortessa flow cytometer (BD).

### Mouse infection models

To evaluate the pathogenesis of V12CBD-bound *S. aureus*, *S. aureus* T23 cells were premixed with 100, 200, and 400 µg/ml of V12CBD in PBS for 30 min, after washing with PBS to remove unbound V12CBD, bacterial cells were injected intraperitoneally into female BALB/c mice under a dose of  $2.5 \times 10^8$  CFU/mouse ( $n = 5$ ). The naïve *S. aureus* without V12CBD treatment was used as the control ( $n = 5$ ).

For the lethal challenge and therapy experiments, female BALB/c mice were infected intraperitoneally with  $2.5 \times 10^8$  CFU of *S. aureus* T23 and received a single dose of 6 mg/kg ( $n = 10$ ), 12 mg/kg V12CBD ( $n = 10$ ), or equal volumes of PBS ( $n = 6$ ) at 3 h post-infection. To assess the prophylactic effect of V12CBD, female BALB/c mice were received intraperitoneal injection at a single dose of 12 mg/kg V12CBD ( $n = 14$ ) or equal volumes of PBS ( $n = 10$ ). Twenty-four hours post-V12CBD injection, mice were received a lethal dose of  $2 \times 10^8$  CFU of *S. aureus* T23.

For studying the bacterial loads in the preventive animal model, female BALB/c mice were pre-received a single dose of 12 mg/kg V12CBD intraperitoneally ( $n = 18$ ) and, 24 h later, challenged with either  $1.3 \times 10^8$  CFU of *S. aureus* T23 ( $n = 8$ ) or  $1 \times 10^{10}$  CFU of *S. aureus* N315 ( $n = 10$ ). Groups pretreated with equal volumes of PBS were used as the controls.

### Illumine library preparation and sequencing

Log phase *S. aureus* T23 was cultured in the presence/absence of 25 µg/ml V12CBD for 4 h at 37°C, and total RNA was extracted using

RNeasy Protect Bacteria Midi Kit (Qiagen). RNA integrity and quantity were checked using an Agilent 2100 Bioanalyzer (Agilent Technologies) and NanoDrop 2000 spectrophotometer (Thermo Scientific). The cDNA libraries were constructed using Illumina TruSeq™ RNA Sample Prep Kit (Illumina). After normalization and dilution, the cDNA libraries were sequenced on Illumina NextSeq™ 5006.2 platform utilizing the NextSeq™ 500 High Output Kit (Illumina).

### Quantitative real-time PCR (qRT-PCR)

qRT-PCR was performed using an Applied Biosystems 7500 Real-time PCR System (Applied Biosystems, USA). Primers used were shown in Appendix Table S2. Total RNA of RAW264.7 and BHK-21 cells was extracted using the TRIzol method as described previously (Rio *et al.*, 2010). The influence of transfected pcDNA3.1-V12CBD on the gene expression levels of BHK-21 cells was examined at 24 and 48 h after transfection, using PBS-treated wells as controls. To explore the possible targeting pathway of V12CBD, RAW264.7 cells were pretreated with various signal pathway inhibitors, including BAY 11-7082 (10 μM, targeting NF-κB pathway), SB203580 (10 μM, targeting p38MAPK pathway), SP600125 (1 μM, targeting JNK pathway), and U012 (10 μM, targeting ERK1/2 pathway) for 30 min, and then cocultured with 50 μg/ml V12CBD for 24 h. Expression levels of the bacterial genes were analyzed using the comparative CT method ( $2^{-\Delta\Delta CT}$ ; Hu *et al.*, 2016). The relative mRNA expression levels (Rel. mRNA) of the gene in macrophage or BHK-21 cells were compared with that of *Gapdh* gene.

### Statistical analysis

Two-tailed Student's *t*-tests were used to compare all *in vitro* assays, including adhesion assay, macrophage assays, and qPCR assays. Bacterial loads in abscess models were analyzed using the non-parametric Mann-Whitney test (two-tailed) for statistical significance. The log-rank test was used for survival analysis in mouse models.

### Accession numbers

The bacterial RNA-Seq data have been deposited in NCBI's Gene Expression Omnibus and are accessible through GEO Series accession number GSE115993.

**Expanded View** for this article is available online.

### Acknowledgements

This work was supported by the National Natural Science Foundation of China (No. 31400126 and No. 31770192 to HY, and No. 31570175 to HP Wei) and the Youth Innovation Promotion Association CAS (to HY). We are grateful to Dr. Xuefang An, Dr. Jia Wu, and Mrs. Juan Min from the Core Facility and Technical Support, Wuhan Institute of Virology, for their assistance in animal experiments and flow cytometry studies. We are grateful to Dr. Bin Wei, Dr. Jianjun Chen, and Dr. Yan Yang from Wuhan Institute of Virology, Chinese Academy of Sciences, as well as Dr. Qing Tang from Huazhong Agricultural University, for their helpful discussions and suggestions on this work.

### Author contributions

HY and HW conceived the study. HY, JX, WL, and JL performed the experiments. HY, SW, JY, YL, and HW analyzed the data. HY and HW wrote the manuscript.

### Conflict of interest

The authors declare that they have no conflict of interest.

## References

- Aktan F (2004) iNOS-mediated nitric oxide production and its regulation. *Life Sci* 75: 639–653
- Barbu EM, Mackenzie C, Foster TJ, Hook M (2014) SdrC induces staphylococcal biofilm formation through a homophilic interaction. *Mol Microbiol* 94: 172–185
- Baron C (2010) Antivirulence drugs to target bacterial secretion systems. *Curr Opin Microbiol* 13: 100–105
- Bayer AS, Coulter SN, Stover CK, Schwan WR (1999) Impact of the high-affinity proline permease gene (*putP*) on the virulence of *Staphylococcus aureus* in experimental endocarditis. *Infect Immun* 67: 740–744
- Beier D, Gross R (2006) Regulation of bacterial virulence by two-component systems. *Curr Opin Microbiol* 9: 143–152
- Boucher HW, Corey GR (2008) Epidemiology of methicillin-resistant *Staphylococcus aureus*. *Clin Infect Dis* 46(Suppl 5): S344–S349
- Casadevall A, Dadachova E, Pirofski LA (2004) Passive antibody therapy for infectious diseases. *Nat Rev Microbiol* 2: 695–703
- Cegelski L, Marshall GR, Eldridge GR, Hultgren SJ (2008) The biology and future prospects of antivirulence therapies. *Nat Rev Microbiol* 6: 17–27
- Coulter SN, Schwan WR, Ng EY, Langhorne MH, Ritchie HD, Westbrook-Wadman S, Hufnagle WO, Folger KR, Bayer AS, Stover CK (1998) *Staphylococcus aureus* genetic loci impacting growth and survival in multiple infection environments. *Mol Microbiol* 30: 393–404
- Cunliffe KM, Lee JC, Frank MM (2001) Capsule production and growth phase influence binding of complement to *Staphylococcus aureus*. *Infect Immun* 69: 6796–6803
- Davidson AL, Chen J (2004) ATP-binding cassette transporters in bacteria. *Annu Rev Biochem* 73: 241–268
- Delaune A, Dubrac S, Blanchet C, Poupel O, Mader U, Hiron A, Leduc A, Fitting C, Nicolas P, Cavaillon JM, Adib-Conquy M, Msadek T (2012) The WalkR system controls major staphylococcal virulence genes and is involved in triggering the host inflammatory response. *Infect Immun* 80: 3438–3453
- DeLeo FR, Chambers HF (2009) Reemergence of antibiotic-resistant *Staphylococcus aureus* in the genomics era. *J Clin Invest* 119: 2464–2474
- DiGiandomenico A, Sellman BR (2015) Antibacterial monoclonal antibodies: the next generation? *Curr Opin Microbiol* 27: 78–85
- Dong Q, Wang J, Yang H, Wei C, Yu J, Zhang Y, Huang Y, Zhang XE, Wei H (2015) Construction of a chimeric lysin Ply187N-V12C with extended lytic activity against staphylococci and streptococci. *Microb Biotechnol* 8: 210–220
- Dubrac S, Boneca IG, Poupel O, Msadek T (2007) New insights into the Walk/WalR (YycG/YycF) essential signal transduction pathway reveal a major role in controlling cell wall metabolism and biofilm formation in *Staphylococcus aureus*. *J Bacteriol* 189: 8257–8269
- Dubrac S, Bisicchia P, Devine KM, Msadek T (2008) A matter of life and death: cell wall homeostasis and the WalkR (YycGF) essential signal transduction pathway. *Mol Microbiol* 70: 1307–1322
- Fabret C, Hoch JA (1998) A two-component signal transduction system essential for growth of *Bacillus subtilis*: implications for anti-infective therapy. *J Bacteriol* 180: 6375–6383
- Fischetti VA (2005) Bacteriophage lytic enzymes: novel anti-infectives. *Trends Microbiol* 13: 491–496

- Foster TJ (2005) Immune evasion by staphylococci. *Nat Rev Microbiol* 3: 948–958
- Fournier B, Philpott DJ (2005) Recognition of *Staphylococcus aureus* by the innate immune system. *Clin Microbiol Rev* 18: 521–540
- Fowler VG Jr, Proctor RA (2014) Where does a *Staphylococcus aureus* vaccine stand? *Clin Microbiol Infect* 20(Suppl 5): 66–75
- Giersing BK, Dastgheyb SS, Modjarrad K, Moorthy V (2016) Status of vaccine research and development of vaccines for *Staphylococcus aureus*. *Vaccine* 34: 2962–2966
- Hu MY, Shen YB, Xu XY, Yu HY, Zhang M, Dang YF, Li JL (2016) Identification, characterization and immunological analysis of Ras related C3 botulinum toxin substrate 1 (Rac1) from grass carp *Ctenopharyngodon idella*. *Dev Comp Immunol* 54: 20–31
- Hua L, Hilliard JJ, Shi Y, Tkaczyk C, Cheng LI, Yu X, Datta V, Ren S, Feng H, Zinsou R, Keller A, O'Day T, Du Q, Cheng L, Damschroder M, Robbie G, Suzich J, Stover CK, Sellman BR (2014) Assessment of an anti-alpha-toxin monoclonal antibody for prevention and treatment of *Staphylococcus aureus*-induced pneumonia. *Antimicrob Agents Chemother* 58: 1108–1117
- Ito T, Katayama Y, Hiramatsu K (1999) Cloning and nucleotide sequence determination of the entire mec DNA of pre-methicillin-resistant *Staphylococcus aureus* N315. *Antimicrob Agents Chemother* 43: 1449–1458
- Jansen KU, Girgenti DQ, Scully IL, Anderson AS (2013) Vaccine review: “*Staphylococcus aureus* vaccines: problems and prospects”. *Vaccine* 31: 2723–2730
- Ji Q, Chen PJ, Qin G, Deng X, Hao Z, Wawrzak Z, Yeo WS, Quang JW, Cho H, Luo GZ, Weng X, You Q, Luan CH, Yang X, Bae T, Yu K, Jiang H, He C (2016) Structure and mechanism of the essential two-component signal-transduction system WalkR in *Staphylococcus aureus*. *Nat Commun* 7: 11000
- Kinkel TL, Roux CM, Dunman PM, Fang FC (2013) The *Staphylococcus aureus* SrrAB two-component system promotes resistance to nitrosative stress and hypoxia. *MBio* 4: e00696–13
- Krachler AM, Orth K (2013) Targeting the bacteria-host interface: strategies in anti-adhesion therapy. *Virulence* 4: 284–294
- Liu J, Zhang X, Yang H, Yuan J, Wei H, Yu J, Fang X (2015) Study of the interactions between endolysin and bacterial peptidoglycan on *S. aureus* by dynamic force spectroscopy. *Nanoscale* 7: 15245–15250
- Loeffler JM, Nelson D, Fischetti VA (2001) Rapid killing of *Streptococcus pneumoniae* with a bacteriophage cell wall hydrolase. *Science* 294: 2170–2172
- Loessner MJ, Wendlinger G, Scherer S (1995) Heterogeneous endolysins in *Listeria monocytogenes* bacteriophages: a new class of enzymes and evidence for conserved holin genes within the siphoviral lysis cassettes. *Mol Microbiol* 16: 1231–1241
- Martin PK, Li T, Sun D, Biek DP, Schmid MB (1999) Role in cell permeability of an essential two-component system in *Staphylococcus aureus*. *J Bacteriol* 181: 3666–3673
- Martinez JL (2008) Antibiotics and antibiotic resistance genes in natural environments. *Science* 321: 365–367
- Miller JF, Mekalanos JJ, Falkow S (1989) Coordinate regulation and sensory transduction in the control of bacterial virulence. *Science* 243: 916–922
- Monack DM, Mueller A, Falkow S (2004) Persistent bacterial infections: the interface of the pathogen and the host immune system. *Nat Rev Microbiol* 2: 747–765
- Mosser DM, Edwards JP (2008) Exploring the full spectrum of macrophage activation. *Nat Rev Immunol* 8: 958–969
- Nelson DC, Schmelcher M, Rodriguez-Rubio L, Klumpp J, Pritchard DG, Dong S, Donovan DM (2012) Endolysins as antimicrobials. *Adv Virus Res* 83: 299–365
- O’Riordan K, Lee JC (2004) *Staphylococcus aureus* capsular polysaccharides. *Clin Microbiol Rev* 17: 218–234
- Pastagia M, Schuch R, Fischetti VA, Huang DB (2013) Lysins: the arrival of pathogen-directed anti-infectives. *J Med Microbiol* 62: 1506–1516
- Proctor RA (2012) Challenges for a universal *Staphylococcus aureus* vaccine. *Clin Infect Dis* 54: 1179–1186
- Projan SJ, Bradford PA (2007) Late stage antibacterial drugs in the clinical pipeline. *Curr Opin Microbiol* 10: 441–446
- Rasko DA, Moreira CG, de Li R, Reading NC, Ritchie JM, Waldor MK, Williams N, Taussig R, Wei S, Roth M, Hughes DT, Huntley JF, Fina MW, Falck JR, Sperandio V (2008) Targeting QseC signaling and virulence for antibiotic development. *Science* 321: 1078–1080
- Rasko DA, Sperandio V (2010) Anti-virulence strategies to combat bacteria-mediated disease. *Nat Rev Drug Discov* 9: 117–128
- Raz A, Serrano A, Lawson C, Thaker M, Alston T, Bournazos S, Ravetch JV, Fischetti VA (2017) Lysibodies are IgG Fc fusions with lysin binding domains targeting *Staphylococcus aureus* wall carbohydrates for effective phagocytosis. *Proc Natl Acad Sci USA* 114: 4781–4786
- Rio DC, Ares M Jr, Hannon GJ, Nilsen TW (2010) Purification of RNA using TRIzol (TRI reagent). *Cold Spring Harb Protoc* 2010: pdb.prot5439
- Saenz JB, Doggett TA, Haslam DB (2007) Identification and characterization of small molecules that inhibit intracellular toxin transport. *Infect Immun* 75: 4552–4561
- Schuch R, Nelson D, Fischetti VA (2002) A bacteriolytic agent that detects and kills *Bacillus anthracis*. *Nature* 418: 884–889
- Schwan WR, Coulter SN, Ng EY, Langhorne MH, Ritchie HD, Brody LL, Westbrook-Wadman S, Bayer AS, Folger KR, Stover CK (1998) Identification and characterization of the PutP proline permease that contributes to *in vivo* survival of *Staphylococcus aureus* in animal models. *Infect Immun* 66: 567–572
- Serbina NV, Salazar-Mather TP, Biron CA, Kuziel WA, Pamer EG (2003) TNF/ $\alpha$ -iNOS-producing dendritic cells mediate innate immune defense against bacterial infection. *Immunity* 19: 59–70
- Spellberg B, Guidos R, Gilbert D, Bradley J, Boucher HW, Scheld WM, Bartlett JG, Edwards J Jr, Infectious Diseases Society of America (2008) The epidemic of antibiotic-resistant infections: a call to action for the medical community from the Infectious Diseases Society of America. *Clin Infect Dis* 46: 155–164
- Starkey M, Lepine F, Maura D, Bandyopadhyaya A, Lesic B, He J, Kitao T, Righi V, Milot S, Tzika A, Rahme L (2014) Identification of anti-virulence compounds that disrupt quorum-sensing regulated acute and persistent pathogenicity. *PLoS Pathog* 10: e1004321
- Stock AM, Robinson VL, Goudreau PN (2000) Two-component signal transduction. *Annu Rev Biochem* 69: 183–215
- Thakker M, Park JS, Carey V, Lee JC (1998) *Staphylococcus aureus* serotype 5 capsular polysaccharide is antiphagocytic and enhances bacterial virulence in a murine bacteremia model. *Infect Immun* 66: 5183–5189
- Thanert R, Goldmann O, Beineke A, Medina E (2017) Host-inherent variability influences the transcriptional response of *Staphylococcus aureus* during *in vivo* infection. *Nat Commun* 8: 14268
- Tong SY, Davis JS, Eichenberger E, Holland TL, Fowler VG Jr (2015) *Staphylococcus aureus* infections: epidemiology, pathophysiology, clinical manifestations, and management. *Clin Microbiol Rev* 28: 603–661
- Ulrich M, Bastian M, Cramton SE, Ziegler K, Pragman AA, Bragonzi A, Memmi G, Wolz C, Schlievert PM, Cheung A, Doring G (2007) The staphylococcal respiratory response regulator SrrAB induces ica gene transcription and polysaccharide intercellular adhesin expression, protecting *Staphylococcus aureus* from neutrophil killing under anaerobic growth conditions. *Mol Microbiol* 65: 1276–1287

- Veldkamp KE, van Strijp JA (2009) Innate immune evasion by staphylococci. *Adv Exp Med Biol* 666: 19–31
- Verhoef J, Mattsson E (1995) The role of cytokines in gram-positive bacterial shock. *Trends Microbiol* 3: 136–140
- Vicente M, Hodgson J, Massidda O, Tonjum T, Henriques-Normark B, Ron EZ (2006) The fallacies of hope: will we discover new antibiotics to combat pathogenic bacteria in time? *FEMS Microbiol Rev* 30: 841–852
- Walsh C (2003) Where will new antibiotics come from? *Nat Rev Microbiol* 1: 65–70
- Wang J, Zhou X, Liu S, Li G, Zhang B, Deng X, Niu X (2015) Novel inhibitor discovery and the conformational analysis of inhibitors of listeriolysin O via protein-ligand modeling. *Sci Rep* 5: 8864
- Wozniak DJ, Tiwari KB, Soufan R, Jayaswal RK (2012) The mcsB gene of the clpC operon is required for stress tolerance and virulence in *Staphylococcus aureus*. *Microbiology* 158: 2568–2576